Clinical, Cosmetic and Investigational Dermatology

Dovepress
Taylor & Francis Group

Open Access Full Text Article

ORIGINAL RESEARCH

Deciphering the Causal Links Among Metabolomics, Ageing Phenotypes, and Pathological Scars: A Two-Sample Mendelian Randomization Study

Kang Wang, Kai Hou, Min Wu, Yiping Wu

Department of Plastic and Cosmetic Surgery, Tongji Hospital, Tongji Medical College, Huazhong University of Science and Technology, Wuhan, 430030, People's Republic of China

Correspondence: Min Wu; Yiping Wu, Department of Plastic and Cosmetic Surgery, Tongji Hospital, Tongji Medical College, Huazhong University of Science and Technology, Wuhan, Hubei, People's Republic of China, Email wumin@hust.edu.cn; tongjiplastic@163.com

Background: Hypertrophic scars (HS) and keloids represent pathological outcomes following cutaneous injury, characterized by complex pathogenesis and suboptimal therapeutic outcomes. The interplay between metabolomics and ageing may offer novel intervention targets for scar formation.

Objective: This study aimed to systematically investigate the causal relationships between blood metabolites, ageing phenotypes (telomere length, epigenetic age), and HS/keloids through Two-sample Mendelian randomization (MR) and Two-step Mediation MR analysis.

Methods: We integrated large-scale GWAS data from European populations, including 1400 blood metabolites (n=8299), telomere length (n=438,351), epigenetic age (n=41,000), HS (2068 cases/465,673 controls), and keloids (4086 cases/1,278,496 controls). Two-sample MR analysis was performed using inverse-variance weighted (IVW) and Wald ratio methods. Steiger's, Cochrane's Q, and MR-Egger tests were applied to exclude reverse causality, heterogeneity, and pleiotropy. Mediation effects of ageing phenotypes were quantified.

Results: The study identified 30 metabolites significantly associated with HS and 49 with keloids. Among ageing phenotypes, telomere length showed positive correlations with both scar types, whereas PhenoAge exhibited negative correlations. Key metabolites such as Eugenol sulfate and Phenylacetylglutamate regulated scar formation through dual pathways involving telomere length and PhenoAge.

Conclusion: This study elucidated the causal metabolite-ageing-scar network through genetic evidence, identifying multiple potential therapeutic targets, including Eugenol sulfate and Phenylacetylglutamate. These findings establish a robust foundation for developing targeted metabolic interventions.

Keywords: ageing phenotypes, hypertrophic scars, keloids, metabolomics, mendelian randomization

Introduction

Skin is the largest organ in the human body, serving as a protective barrier for underlying fat, muscles, internal organs, bones, and other structures.[1,2] Yet, the varieties of damaging external stimuli can lead to skin injury, such as surgery, burns, or trauma. Especially, scar formation often occurs following skin injury.[3] Abnormal scars can cause cosmetic defects, physical discomfort, and functional limitations, consequently imposing a significant physiological and psychological burden on patients.[4] Abnormal scars mainly include hypertrophic scars (HS) and keloids. HS and keloids are both associated with disordered deposition of extracellular matrix. HS forms at the origin site of skin injury, and typically does not exceed the wound margins. Keloids, however, extend beyond the wound boundaries and invade surrounding normal tissue.[5] Pathological scars are triggered by multiple factors, including genetic predisposition,[6] mechanical stress,[7]

https://doi.org/10.2147/CCID.S598554
Received: 5 February 2026
Accepted: 30 April 2026
Published: 11 May 2026

inflammation,[8] systemic factors such as sex hormones,[9] and environmental factors like smoking and diet.[10] However, the detailed mechanisms remain to be further explored. The main treatment options for pathological scars include laser therapy, surgical excision, radiotherapy, intralesional 5-fluorouracil injections, and corticosteroid injections.[5,11] However, the overall therapeutic effect remains unsatisfactory, despite these advances. Therefore, identifying novel therapeutic targets would be clinically significant.

Metabolomics is emerging as a novel panacea for identifying key metabolites or metabolic pathways in the domain of fundamental research and drug target discovery.[12] Metabolomics has huge potential in screening targeted metabolites in HS and keloids.[13,14] For instance, arginine metabolism can influence the radiotherapy sensitivity of keloids.[15] However, whether there is a direct or indirect causal relationship between the metabolites and the skin scarring disease remains relatively unclear.

Ageing is a natural process that manifests as a progressive decline in physiological function and increased susceptibility to disease over time.[16] Recent evidence suggests that ageing may serve as a mediator between metabolites and pathological scars. To date, over 400 ageing-related metabolites have been identified,[17] and can be categorized into 7 primary pathways, including lipids and lipoproteins, steroid hormones, renal systems and excretion, amino acids and muscle, diet, oxidative stress and inflammation.[18] Furthermore, ageing has been demonstrated to play a progressive role in various fibrotic diseases, including idiopathic pulmonary fibrosis[19] and renal fibrosis.[20] Similarly, ageing also significantly influences wound healing and scar formation.[21,22] However, it remains insufficiently explored whether potential causal relationships exist between metabolites and ageing, as well as between ageing and pathological scars.

Mendelian randomization (MR) is a statistical method employed in epidemiological research, using genetic variation associated with the exposure factors as instrumental variables (IVs) to infer causal relationships.[23] Genetic variants are determined at birth, and are unaffected by disease status or environmental factors, without producing reverse causality and confounding factors.[24] Although the relationship between metabolites and HS/keloids has been preliminarily explored,[25] we have innovatively investigated the mediating role of ageing.

In terms of this background, therefore, this study aimed to explore the causal relationships between metabolites, ageing, and HS/keloids by two-sample MR analysis. This study systematically investigated the causal effects of 1400 blood metabolites and metabolite ratios on HS and keloids, while assessing the mediating roles of telomere length and epigenetic ageing biomarkers. To ensure robust causal inference, genetic instruments for metabolites were selected, followed by rigorous sensitivity analyses, including Steiger's filter for directionality and assessments of heterogeneity and horizontal pleiotropy. The potential mediating effects of 4 ageing phenotypes, including telomere length, PhenoAge, GrimAge, and Intrinsic Epigenetic Age Acceleration (IEAA), were quantified by integrating their genetically proxied associations with both the identified significant metabolites and the scarring outcomes.

These findings establish a foundation for developing targeted metabolic interventions, advancing scar treatment toward precision metabolic modulation.

Materials and Methods

Study Outline

We employed MR to assess potential causal relationships between blood metabolites, metabolite ratios, and scarring disorders (HS and keloids), while investigating the mediating roles of ageing biomarkers (telomere length, epigenetic age) in these associations (Figure 1). The three core hypotheses of the MR study are: 1) SNPs exhibit robust associations with blood metabolites and metabolite ratios; 2) IVs are unaffected by known confounding factors; 3) IVs influence outcomes exclusively through the specified exposures.

GWAS Data Sources and Data Characteristics

The Genome-Wide Association Study (GWAS) summary statistics for 1091 metabolites and 309 metabolite ratios were obtained from the study by Qin et al,[26] which were derived from a European-ancestry cohort of 8299 individuals. These data are publicly accessible in the GWAS Catalog database (https://www.ebi.ac.uk/gwas/; ID range GCST90199621–GCST90201020).

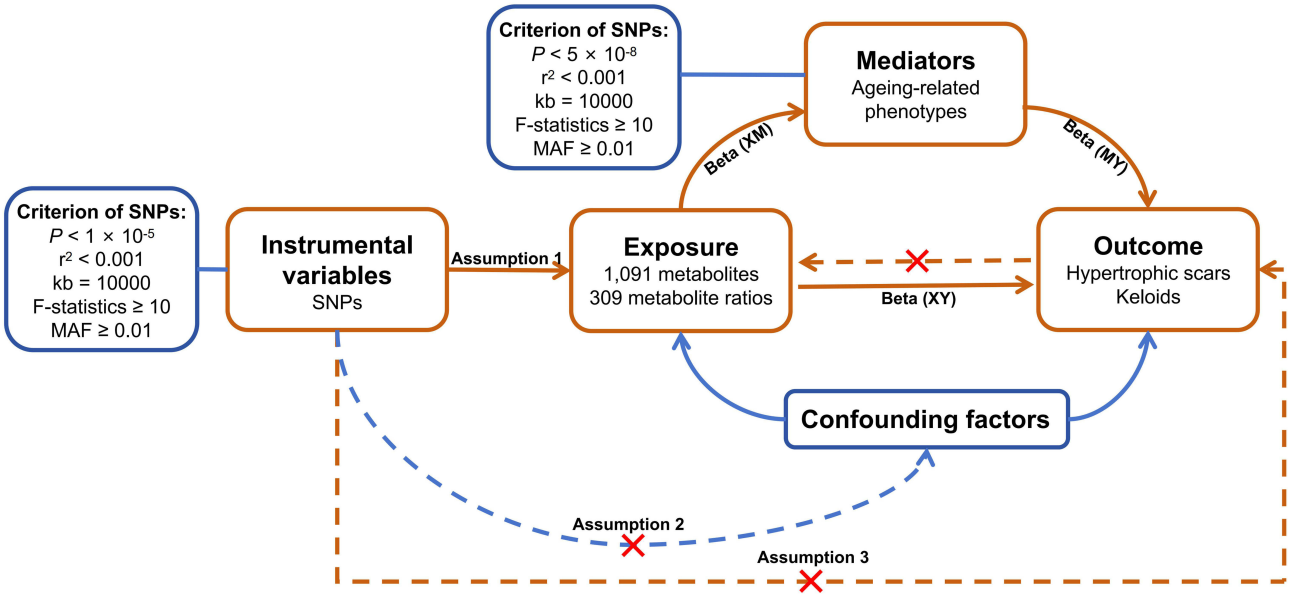

Figure 1 Research Flowchart.

Telomere length and epigenetic age (PhenoAge, GrimAge, IEAA) were selected as ageing-related phenotypes. Genetic data of telomere length were obtained from the GWAS Catalog database (ID GCST90435144). This large-scale dataset comprises information from 438,351 individuals of European ancestry. Genetic data of epigenetic age were derived from the study by McCartney et al,[27] comprising a multi-ethnic dataset of over 41,000 individuals from 29 European-ancestry, 7 African-American, and one Hispanic study cohorts. The European-ancestry subset was utilized for subsequent MR analysis.

The GWAS summary statistics for HS were derived from the FinnGen database (Release R12). The FinnGen database is a large-scale, nationwide cohort that integrates genetic data with longitudinal electronic health records from biobanks and national registries, focusing on European-ancestry participants with disease endpoints defined by ICD-10 codes. The dataset comprises 2068 cases of HS and 465,673 matched controls. The GWAS summary statistics for keloids were sourced from the GWAS Catalog (ID GCST90652488), including 4086 cases and 1,278,496 controls of European ancestry.

Instrumental Variable Selection

Where metabolite levels served as exposures, a significance threshold of $P < 1\times10^{-5}$ was adopted for the selection of IVs, to ensure the inclusion of a sufficient number of genetic IVs. Meanwhile, considering the potential bias introduced by linkage disequilibrium (LD) among Single Nucleotide Polymorphisms (SNPs), strict LD parameters were adopted. SNPs that exhibited an LD threshold of $r^2 < 0.001$, and had a minimum physical distance of 10,000 kilobases (kb) between each other were retained. The implementation of stringent LD clumping criteria ensured independence among selected genetic variants while effectively reducing correlated genetic influences. When ageing-related phenotypes were used as exposures, the significance threshold for IVs was set at $P < 5\times10^{-8}$, with LD pruning criteria of $r^2 < 0.001$ and a physical distance of 10,000 kb applied.

To address potential biases associated with the relatively lenient statistical thresholds used for IV selection, F-statistics were calculated to evaluate both sample overlap effects and weak instrument bias. IVs exhibiting $F < 10$ were excluded due to weak instrument bias. Additionally, to minimize confounding from rare genetic variants, all SNPs with minor allele frequencies (MAF) below 0.01 were systematically excluded from the analysis. The F-statistic was computed as follows.

$$F = \frac{R^2(n-2)}{1-R^2}$$

https://doi.org/10.2147/CCID.S598554

R^2 represents the explanatory power of the SNPs, which can be automatically computed by the TwoSampleMR package, and n denotes the number of SNPs. The MAF was determined as MAF = min (p,1−p), where p is the effect allele frequency of the variant in the reference population.

Mendelian Randomization Analysis

R software and the TwoSampleMR package were used in the two-sample MR analyses. The causal relationship between exposure and outcome was assessed using the inverse-variance weighted (IVW) method when two or more SNPs were included, while the Wald ratio method was applied to analyses involving only one SNP. Additionally, Steiger's filter approach was applied to assess potential reverse causality between exposure and outcome. A Steiger's $P < 0.05$ indicated the absence of significant reverse causation, and this methodological framework ensures robust causal inference while accounting for directional pleiotropy and instrument validity.

In MR analyses, the IVW method integrates effect estimates to balance statistical power and bias control while accounting for inter-variant heterogeneity, thereby maximizing statistical efficiency and mitigating weak instrument bias. The Wald ratio method directly estimates causal effects by computing the ratio of SNP-outcome to SNP-exposure associations. The Steiger's test uniquely evaluates causal directionality by comparing the variance explained by SNPs in exposure versus outcome. Together, these methods form an analytical framework that ensures both methodological rigor and biological plausibility in causal inference.

Sensitivity Analysis

To enhance the robustness of our findings and mitigate potential false positives, we conducted comprehensive sensitivity analyses, including assessments of heterogeneity and horizontal pleiotropy. Heterogeneity was evaluated using Cochrane's Q test, with a Q statistic $P > 0.05$ indicated the absence of significant heterogeneity. Horizontal pleiotropy was examined via the MR-Egger intercept test, where an intercept $P > 0.05$ suggested no evidence of directional pleiotropy. These analytical steps collectively strengthened the validity of our causal inferences by addressing key assumptions in Mendelian randomization.

Results

Hypertrophic Scar

MR Results of Metabolites and Hypertrophic Scars

The selected SNPs associated with metabolites were listed in Table S1. All included SNPs demonstrated strong associations with the metabolites, with F-statistics > 10 and MAF > 0.01, indicating minimal weak instrument bias and exclusion of confounding by rare genetic variants.

Firstly, MR analysis identified 30 metabolites with potential causal relationships with HS. Among these, 11 metabolites exhibited protective effects (OR < 1), while 19 metabolites showed risk-promoting effects on HS (OR > 1) (Figure 2 and Table S2). The Steiger's directionality test confirmed the absence of reverse causation for 30 metabolites on HS, robustly supporting our prespecified causal model where metabolic alterations influence HS rather than vice versa (Table S3A. Moreover, the MR analysis also revealed three exposures with significant protective effects against HS: Cysteine levels [GCST90200439] (OR 0.71, 95% CI: 0.56–0.91, $P = 0.006$), Leucine to N-palmitoyl-sphingosine [GCST90200972] (d18:1 to 16:0) ratio (OR 0.74, 95% CI: 0.61–0.90, $P = 0.003$), and Taurine to cysteine ratio [GCST90200893] (OR 0.80, 95% CI: 0.66–0.98, $P = 0.028$). Conversely, the analysis identified three exposures with statistically significant risk-enhancing effects on HS formation: X-22776 levels [GCST90200595] (OR 1.38, 95% CI: 1.07–1.79, P = 0.014), Tridecenedioate (C13:1-DC) levels [GCST90199867] (OR 1.34, 95% CI: 1.08–1.66, P = 0.008), and Phosphate-to-phosphoethanolamine ratio [GCST90200766] (OR 1.32, 95% CI: 1.04–1.67, P = 0.022).

All sensitivity analyses yielded $P > 0.05$ for both heterogeneity (Cochrane's Q) and horizontal pleiotropy (MR-Egger intercept), indicating no detectable heterogeneity or directional pleiotropy among the IVs (Table S3B and C). These findings substantially reinforce the robustness and validity of our MR estimates.

A

Exposure	Outcome	Method	SNPs	MR.Pval	OR (95% CI)
Cysteine levels	Hypertrophic Scar	IVW	14	0.006	0.712 (0.560 to 0.907)
Leucine to N−palmitoyl−sphingosine (d18:1 to 16:0) ratio	Hypertrophic Scar	IVW	22	0.003	0.740 (0.608 to 0.900)
Taurine to cysteine ratio	Hypertrophic Scar	IVW	19	0.028	0.799 (0.655 to 0.976)
3−carboxy−4−methyl−5−propyl−2−furanpropanoate (cmpf) levels	Hypertrophic Scar	IVW	16	0.036	0.801 (0.651 to 0.986)
Aspartate to mannose ratio	Hypertrophic Scar	IVW	20	0.018	0.811 (0.681 to 0.965)
Vanillic acid glycine levels	Hypertrophic Scar	IVW	20	0.017	0.818 (0.694 to 0.965)
Gamma−glutamylglutamate levels	Hypertrophic Scar	IVW	26	0.045	0.833 (0.696 to 0.996)
Trans−urocanate levels	Hypertrophic Scar	IVW	18	0.016	0.840 (0.729 to 0.967)
X−07765 levels	Hypertrophic Scar	IVW	23	0.042	0.847 (0.723 to 0.994)
X−24811 levels	Hypertrophic Scar	IVW	26	0.044	0.855 (0.734 to 0.996)
X−11858 levels	Hypertrophic Scar	IVW	27	0.047	0.873 (0.763 to 0.998)

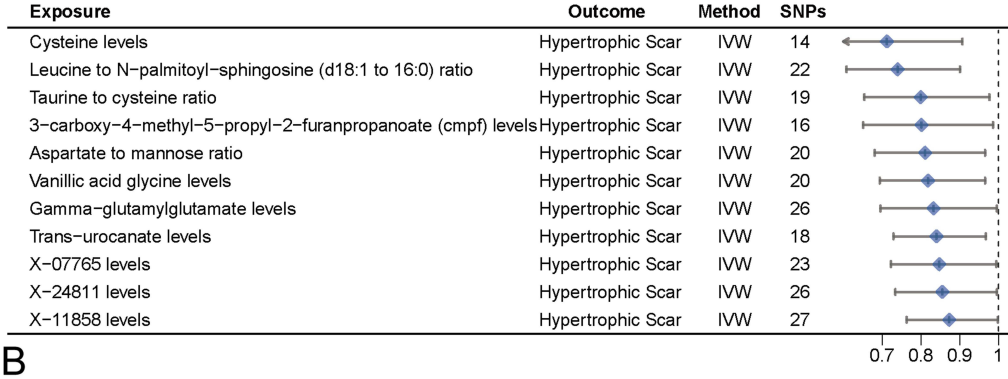

B

Exposure	Outcome	Method	SNPs	MR.Pval	OR (95% CI)
Octadecanedioylcarnitine (C18−DC) levels	Hypertrophic Scar	IVW	23	0.034	1.121 (1.009 to 1.246)
Octadecenedioate (C18:1−DC) levels	Hypertrophic Scar	IVW	22	0.027	1.144 (1.015 to 1.290)
N−acetylglycine levels	Hypertrophic Scar	IVW	22	0.042	1.154 (1.005 to 1.324)
N−acetylglucosamine/n−acetylgalactosamine levels	Hypertrophic Scar	IVW	16	0.036	1.177 (1.011 to 1.371)
P−cresol glucuronide levels	Hypertrophic Scar	IVW	21	0.045	1.200 (1.004 to 1.435)
2−naphthol sulfate levels	Hypertrophic Scar	IVW	22	0.012	1.213 (1.043 to 1.411)
Glycosyl−N−palmitoyl−sphingosine (d18:1/16:0) levels	Hypertrophic Scar	IVW	22	0.005	1.222 (1.061 to 1.407)
Aconitate [cis or trans] levels	Hypertrophic Scar	IVW	21	0.046	1.245 (1.004 to 1.544)
S−allylcysteine levels	Hypertrophic Scar	IVW	16	0.013	1.249 (1.048 to 1.490)
Alanine levels	Hypertrophic Scar	IVW	22	0.023	1.253 (1.032 to 1.521)
X−26111 levels	Hypertrophic Scar	IVW	20	0.004	1.254 (1.075 to 1.463)
X−23655 levels	Hypertrophic Scar	IVW	23	0.004	1.263 (1.077 to 1.482)
S−carboxyethylcysteine levels	Hypertrophic Scar	IVW	22	0.009	1.267 (1.060 to 1.516)
Histidine to pyruvate ratio	Hypertrophic Scar	IVW	20	0.011	1.292 (1.060 to 1.573)
X−17351 levels	Hypertrophic Scar	IVW	17	0.006	1.299 (1.076 to 1.569)
Stachydrine levels	Hypertrophic Scar	IVW	22	0.009	1.300 (1.066 to 1.586)
Phosphate to phosphoethanolamine ratio	Hypertrophic Scar	IVW	14	0.022	1.318 (1.041 to 1.669)
Tridecenedioate (C13:1−DC) levels	Hypertrophic Scar	IVW	20	0.008	1.337 (1.079 to 1.658)
X−22776 levels	Hypertrophic Scar	IVW	11	0.014	1.383 (1.067 to 1.794)

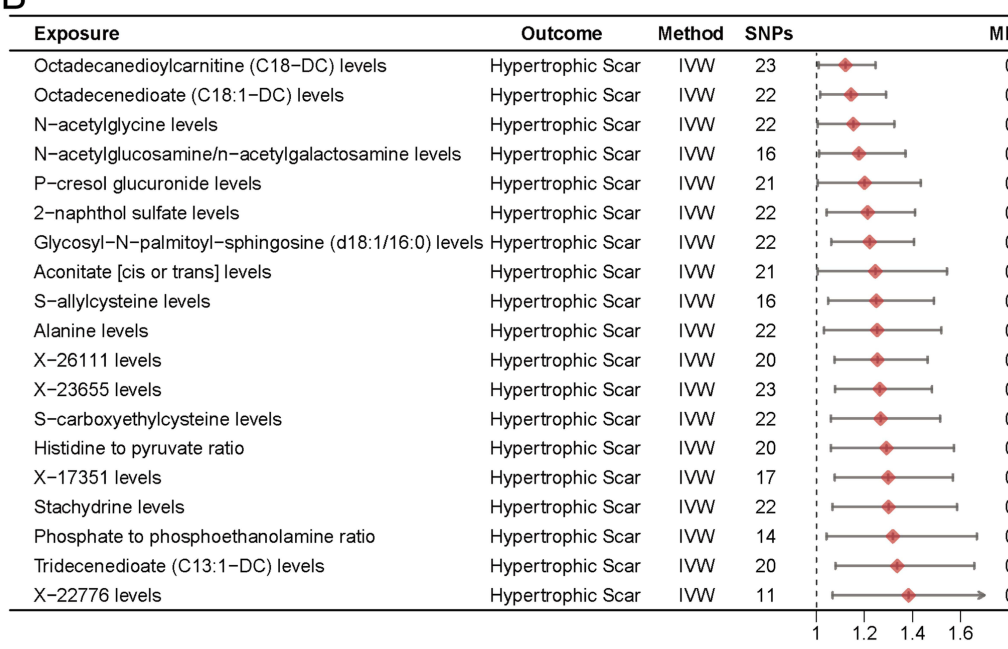

Figure 2 Forest plots of the association between metabolites and hypertrophic scars (HS). (**A**) Forest plot of 11 metabolites inhibiting HS. (**B**) Forest plot of 19 metabolites promoting HS.

MR Results of Ageing and Hypertrophic Scars

The principles for selecting SNPs associated with ageing were as previously described, with the results of the selected SNPs shown in Table S4. MR results revealed potential causal relationships between telomere length, PhenoAge, and IEAA with HS (Figure 3 and Table S5). Notably, telomere length exhibited a positive correlation with HS (OR 1.327, 95% CI: 1.09–1.603, $P = 0.003$), indicating that telomere shortening might reduce the risk of developing HS. Conversely, both PhenoAge and IEAA exhibited negative causal effects on HS (PhenoAge: OR 0.911, 95% CI: 0.848–0.979, $P = 0.011$; IEAA: OR 0.926, 95% CI: 0.878–0.976, $P = 0.004$), indicating that accelerated epigenetic ageing might reduce the

Mediation	Outcome	Method	SNPs	MR.Pval	OR (95% CI)
Telomere Length	Hypertrophic Scar	IVW	192	0.003	1.327 (1.099 to 1.603)
PhenoAge	Hypertrophic Scar	IVW	11	0.011	0.911 (0.848 to 0.979)
GrimAge	Hypertrophic Scar	IVW	4	0.904	0.988 (0.811 to 1.203)
IEAA	Hypertrophic Scar	IVW	24	0.004	0.926 (0.878 to 0.976)

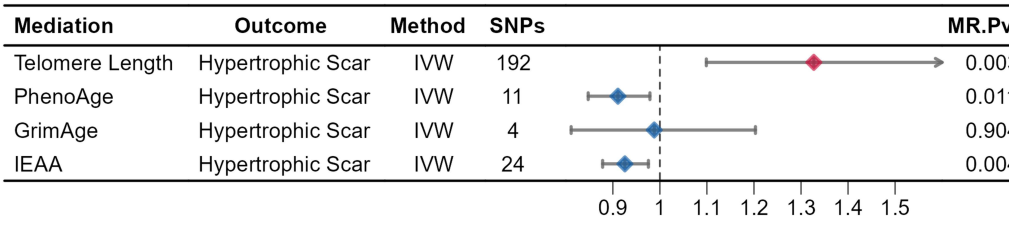

Figure 3 Forest plot of the association between ageing phenotypes and HS.

https://doi.org/10.2147/CCID.S598554

HS risk. No significant association was observed between GrimAge and HS. These findings suggested that ageing may reduce the formation risk of HS.

Sensitivity analyses demonstrated no significant heterogeneity or horizontal pleiotropy ($P > 0.05$) in the MR assessments of telomere length, PhenoAge, GrimAge, and IEAA with HS (Table S6A and B). These results further confirmed the reliability of our causal inferences regarding ageing biomarkers and HS pathogenesis.

MR Results of Metabolites and Ageing

Metabolites and Telomere Length

MR analysis results indicated that 90 metabolites exhibited a potential causal relationships with telomere length. Among these, 52 metabolites showed a negative correlations with telomere length (OR < 1), while 38 metabolites demonstrated a positive correlation (OR > 1) (Figure 4 and Table S7). Notably, three metabolites also exerted significant effects on HS. After excluding results with inconsistent directionality, one metabolite (X-17351 [GCST90200560]) was ultimately identified as being related to HS and involving telomere length. Cases with consistent directionality were illustrated in Figure S1. The Steiger's directionality test results indicated that none of these 88 metabolites showed an inverse causal relationship with telomere length (Table S8A).

In the sensitivity analysis, heterogeneity and pleiotropy tests revealed no evidence of either heterogeneity or pleiotropy in the dataset used for the MR analysis (Table S8B and C). This finding indicated that the results of our MR analysis were robust and reliable.

Metabolites and PhenoAge

According to the MR results, there were 58 metabolites with a potential causal relationships with PhenoAge (Figure 5 and Table S7). Of these, 28 metabolites exhibited negative correlations with PhenoAge (OR < 1), while 30 metabolites showed positive correlations (OR > 1). Intriguingly, after excluding results with inconsistent directionality, N-acetylglycine (GCST90199688) emerged as a dual-pathway mediator, exhibiting both direct effects on HS and indirect

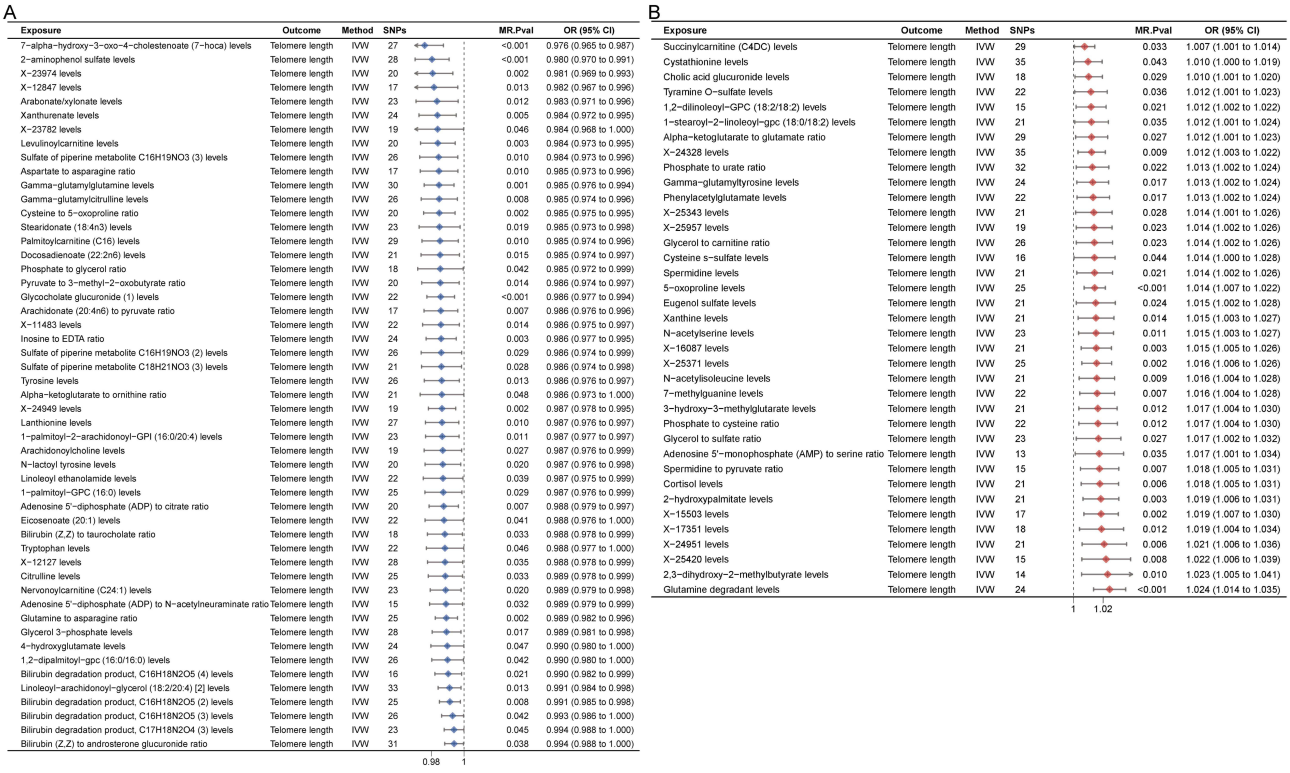

Figure 4 Forest plots of the association between metabolites and telomere length. (**A**) Forest plot of 52 metabolites negative correlated with telomere length. (**B**) Forest plot of 38 metabolites positive correlated with telomere length.

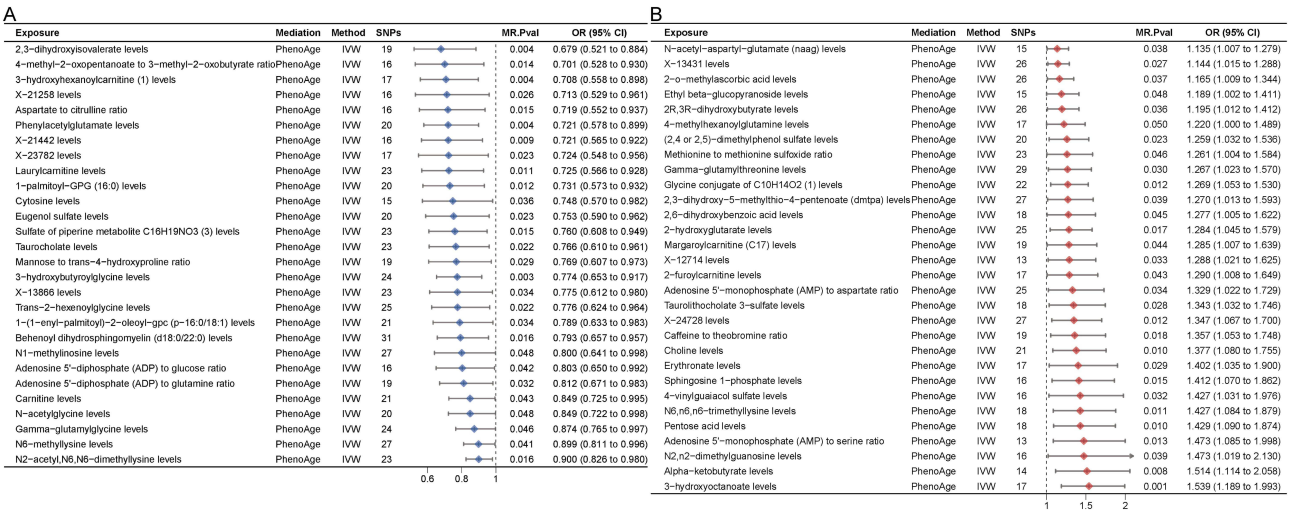

Figure 5 Forest plots of the association between metabolites and PhenoAge. (**A**) Forest plot of 28 metabolites negative correlated with PhenoAge. (**B**) Forest plot of 30 metabolites positive correlated with PhenoAge.

effects through PhenoAge modulation. The directionality consistency is illustrated in Figure S1. The remaining 57 metabolites influenced HS exclusively through PhenoAge mediation. Steiger's directionality tests confirmed the absence of reverse causation for all 58 metabolite-PhenoAge associations, thereby establishing unidirectional metabolic-epigenetic-scarring pathways (Table S8).

The results of heterogeneity and pleiotropy tests in the sensitivity analysis indicated that neither heterogeneity nor pleiotropy existed in the data used for the MR analysis (Table S8), confirming the reliability of our MR findings.

Metabolites and IEAA

The MR analysis revealed that 63 metabolites exhibited potential causal relationships with IEAA (Figure 6 and Table S7). Among these, 28 metabolites showed negative correlations with IEAA (OR < 1), while 35 metabolites demonstrated positive correlations (OR > 1). These 63 metabolites could only influence HS by affecting IEAA. Steiger's directionality test results indicated that no reverse causal relationship existed between these 63 metabolites and IEAA (Table S8). The results of the heterogeneity test and the pleiotropy test corroborate the reliability of the MR analysis findings (Table S8).

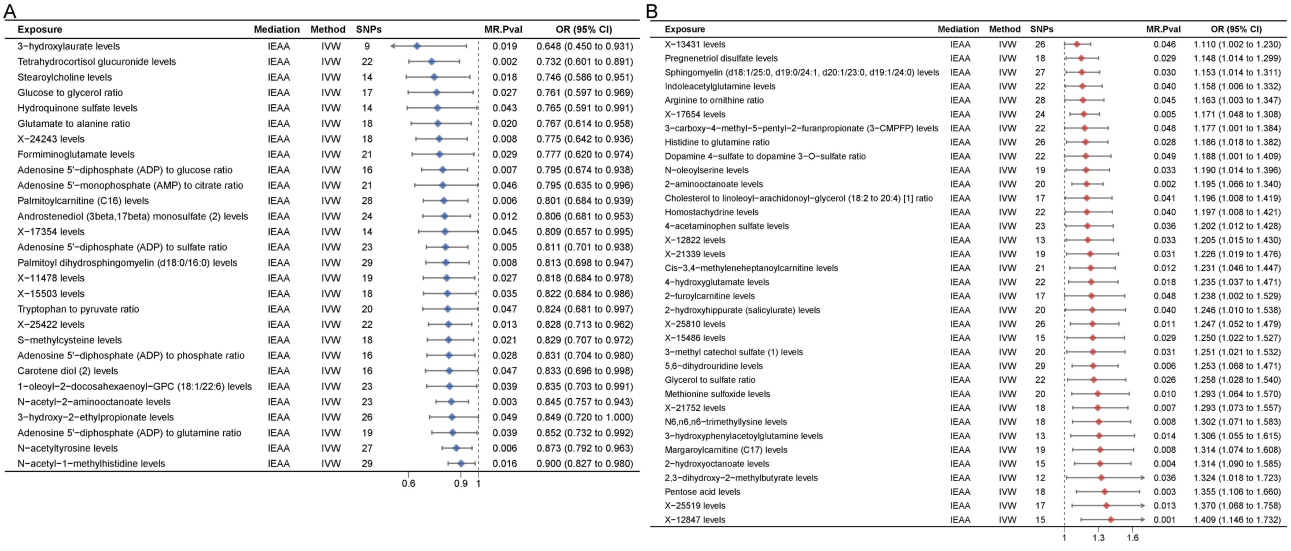

Figure 6 Forest plots of the association between metabolites and Intrinsic Epigenetic Age Acceleration (IEAA). (**A**) Forest plot of 28 metabolites negative correlated with IEAA. (**B**) Forest plot of 35 metabolites positive correlated with IEAA.

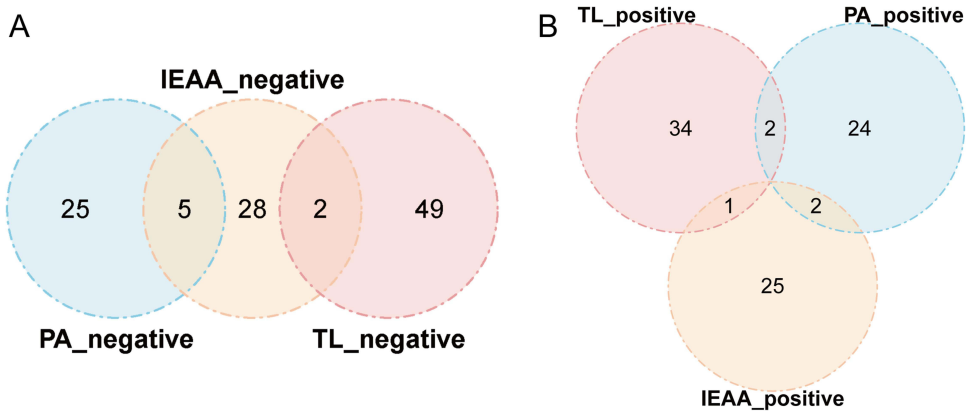

Figure 7 Venn diagram of the intersection metabolites with causal relationships to telomere length, PhenoAge, and IEAA. (**A**) Intersection metabolites with negative association to telomere length, PhenoAge, and IEAA. (**B**) Intersection metabolites with positive association to telomere length, PhenoAge, and IEAA.

Key Metabolites Screening in Biological Ageing

Intersection analysis of metabolites causally linked to telomere length, PhenoAge, and IEAA identified 12 key regulators influencing HS through ≥2 ageing phenotypes (Figure 7), with details of 12 metabolites presented in Table 1. In particular, the adenosine 5′-diphosphate (ADP) to glucose ratio, ADP-to-glutamine ratio, X-15503, Eugenol sulfate, and Phenylacetylglutamate were 5 metabolites positively correlated with HS. It means that reduced levels of these metabolites could alleviate HS formation by promoting ageing. Margaroylcarnitine (C17), 2-furoylcarnitine, pentose acid, N6,n6,n6-trimethyllysine, X-13431, 4-hydroxyglutamate, X-12847 were 7 metabolites negatively correlated with HS. This meant the elevated levels of these metabolites may attenuate HS by accelerating biological ageing processes. The mediating effects of the above 12 metabolites were presented in Table 2. The calculation method for the mediation effects is as follows: Beta = Beta(XM) × Beta(MY).

Table 1 The 12 Key Regulators Influencing HS Through Ageing Phenotypes

GWAS ID	Met	Change	GWAS ID	Met	Change
GCST90199929	Margaroylcarnitine (C17) levels	Negative	GCST90200516	X-12847 levels	Negative
GCST90200155	2-furoylcarnitine levels	Negative	GCST90200947	Adenosine 5'-diphosphate (ADP) to glucose ratio	Positive
GCST90200259	Pentose acid levels	Negative	GCST90200962	ADP to glutamine ratio	Positive
GCST90200344	N6,n6,n6-trimethyllysine levels	Negative	GCST90200543	X-15503 levels	Positive
GCST90200710	X-13431 levels	Negative	GCST90199986	Eugenol sulfate levels	Positive
GCST90199890	4-hydroxyglutamate levels	Negative	GCST90200069	Phenylacetylglutamate levels	Positive

Table 2 The Mediation Effect of 12 Key Metabolites Influencing HS

Exposure	Mediation	Outcome	Effect
4-hydroxyglutamate levels	Telomere length	Hypertrophic Scar	−0.00291
4-hydroxyglutamate levels	IEAA	Hypertrophic Scar	−0.0163
X-12847 levels	Telomere length	Hypertrophic Scar	−0.00524
X-12847 levels	IEAA	Hypertrophic Scar	−0.0265
Margaroylcarnitine (C17) levels	PhenoAge	Hypertrophic Scar	−0.0234
Margaroylcarnitine (C17) levels	IEAA	Hypertrophic Scar	−0.0211
2-furoylcarnitine levels	PhenoAge	Hypertrophic Scar	−0.0238
2-furoylcarnitine levels	IEAA	Hypertrophic Scar	−0.0165
Pentose acid levels	PhenoAge	Hypertrophic Scar	−0.0334

(*Continued*)

Table 2 (Continued).

Exposure	Mediation	Outcome	Effect
Pentose acid levels	IEAA	Hypertrophic Scar	−0.0235
N6,n6,n6-trimethyllysine levels	PhenoAge	Hypertrophic Scar	−0.0333
N6,n6,n6-trimethyllysine levels	IEAA	Hypertrophic Scar	−0.0204
X-13431 levels	PhenoAge	Hypertrophic Scar	−0.0125
X-13431 levels	IEAA	Hypertrophic Scar	−0.00808
Eugenol sulfate levels	Telomere length	Hypertrophic Scar	0.00423
Eugenol sulfate levels	PhenoAge	Hypertrophic Scar	0.0265
Phenylacetylglutamate levels	Telomere length	Hypertrophic Scar	0.00375
Phenylacetylglutamate levels	PhenoAge	Hypertrophic Scar	0.0306
X-15503 levels	Telomere length	Hypertrophic Scar	0.00524
X-15503 levels	IEAA	Hypertrophic Scar	0.0152
ADP to glucose ratio	PhenoAge	Hypertrophic Scar	0.0205
ADP to glucose ratio	IEAA	Hypertrophic Scar	0.0177
ADP to glutamine ratio	PhenoAge	Hypertrophic Scar	0.0195
ADP to glutamine ratio	IEAA	Hypertrophic Scar	0.0123

Keloid

MR Results of Metabolites and keloid

MR results revealed 49 metabolites with potential causal relationships to keloids (Figure 8 and Table S9). Of these, 26 metabolites exhibited a negative correlation with keloids (OR < 1), while 23 metabolites showed a positive correlation (OR > 1). Steiger's directionality test results indicated that no reverse causal relationship existed (Table S10A). Herein, the three exposure factors exhibiting the strongest negative correlation were: 4-methyl-2-oxopentanoate to 3-methyl-2-oxobutyrate ratio [GCST90201017] (OR 0.773, 95% CI: 0.645–0.928, $P = 0.006$), Branched-chain, straight-chain, or cyclopropyl 10:1 fatty acid (1) levels [GCST90200251] (OR 0.789, 95% CI: 0.653–0.953, $P = 0.014$), 4-hydroxyglutamate levels [GCST90199890] (OR 0.799, 95% CI: 0.708–0.901, $P < 0.001$). The three exposure factors exhibiting the strongest positive correlation were: 4-methyl-2-oxopentanoate levels [GCST90199655] (OR 1.414, 95% CI: 1.178–1.697, $P < 0.001$), 2,3-dihydroxy-2-methylbutyrate levels [GCST90200112] (OR 1.333, 95% CI: 1.107–1.606, $P = 0.002$), X-25957 levels [GCST90200660] (OR 1.307, 95% CI: 1.115–1.531, $P < 0.001$).

The results of the heterogeneity and pleiotropy tests in the sensitivity analysis, with $P > 0.05$, indicated that the data used in the MR analysis exhibit neither heterogeneity nor pleiotropy (Table S10B and C), demonstrating the reliability of the MR analysis results.

MR Results of Ageing and Keloid

The MR analysis results for ageing and keloids were presented in Figure 9. Telomere length and PhenoAge exhibited a potential causal relationship with keloids (Table S11). Specifically, telomere length showed a positive correlation with keloids, meaning that telomere shortening reduced the risk of developing keloids. PhenoAge exhibited a negative correlation with keloids, meaning accelerated PhenoAge reduced the risk of developing keloids. However, neither GrimAge nor IEAA demonstrated significant correlation with keloid pathogenesis. Sensitivity analyses confirmed the absence of significant heterogeneity or horizontal pleiotropy (Table S12A and B), thereby substantiating the reliability of our MR estimates.

MR Results of Metabolites and Ageing

Telomere Length

Previous MR analysis identified 90 metabolites associated with telomere length (Figure 4 and Table S7). Of these, eight metabolites also exhibited significant effects on keloid. Following directional profiling (Figure S1), a total of 5 metabolites (4-hydroxyglutamate [GCST90199890], 2,3-dihydroxy-2-methylbutyrate [GCST90200112], Nervonoylcarnitine (C24:1) [GCST90200143], 3-hydroxy-3-methylglutarate [GCST90200298], X-25957

A

Exposure	Outcome	Method	SNPs	MR.Pval	OR (95% CI)
4−methyl−2−oxopentanoate to 3−methyl−2−oxobutyrate ratio	Keloids	IVW	18	0.006	0.773 (0.645 to 0.928)
Branched−chain, straight−chain, or cyclopropyl 10:1 fatty acid (1) levels	Keloids	IVW	12	0.014	0.789 (0.653 to 0.953)
4−hydroxyglutamate levels	Keloids	IVW	24	<0.001	0.799 (0.708 to 0.901)
Aspartate to citrulline ratio	Keloids	IVW	17	0.005	0.805 (0.692 to 0.938)
Stearate (18:0) levels	Keloids	IVW	18	0.036	0.827 (0.693 to 0.988)
X−12680 levels	Keloids	IVW	18	0.020	0.834 (0.715 to 0.972)
Cysteine levels	Keloids	IVW	14	0.047	0.834 (0.698 to 0.997)
4−methoxyphenol sulfate levels	Keloids	IVW	19	0.028	0.844 (0.726 to 0.982)
Adenosine 5'−monophosphate (AMP) to tyrosine ratio	Keloids	IVW	18	0.029	0.850 (0.735 to 0.983)
Picolinoylglycine levels	Keloids	IVW	21	0.023	0.851 (0.740 to 0.978)
Furaneol sulfate levels	Keloids	IVW	13	0.032	0.853 (0.737 to 0.986)
X−25420 levels	Keloids	IVW	15	0.050	0.853 (0.727 to 1.000)
Tyramine O−sulfate levels	Keloids	IVW	22	0.021	0.854 (0.747 to 0.976)
Vanillic acid glycine levels	Keloids	IVW	20	0.027	0.863 (0.757 to 0.984)
N−palmitoyl−sphingosine (d18:1 to 16:0) to N−palmitoyl−sphinganine (d18:0 to 16:0) ratio	Keloids	IVW	20	0.023	0.865 (0.763 to 0.980)
Beta−hydroxyisovaleroylcarnitine levels	Keloids	IVW	33	0.008	0.871 (0.785 to 0.965)
Sulfate of piperine metabolite C18H21NO3 (1) levels	Keloids	IVW	23	0.048	0.873 (0.763 to 0.999)
X−18901 levels	Keloids	IVW	25	0.045	0.881 (0.778 to 0.997)
Nervonoylcarnitine (C24:1) levels	Keloids	IVW	24	0.012	0.881 (0.799 to 0.972)
Phosphate to tyrosine ratio	Keloids	IVW	30	0.046	0.885 (0.786 to 0.998)
5−hydroxymethyl−2−furoylcarnitine levels	Keloids	IVW	22	0.042	0.895 (0.804 to 0.996)
X−17654 levels	Keloids	IVW	26	0.010	0.898 (0.828 to 0.975)
Cys−gly, oxidized levels	Keloids	IVW	25	0.016	0.901 (0.828 to 0.981)
1−stearoyl−2−oleoyl−GPE (18:0/18:1) levels	Keloids	IVW	26	0.034	0.904 (0.824 to 0.992)
N−succinyl−phenylalanine levels	Keloids	IVW	26	0.036	0.918 (0.848 to 0.994)
X−19141 levels	Keloids	IVW	24	0.035	0.929 (0.868 to 0.995)

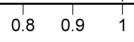

B

Exposure	Outcome	Method	SNPs	MR.Pval	OR (95% CI)
2−hydroxy−4−(methylthio)butanoic acid levels	Keloids	IVW	24	0.044	1.087 (1.002 to 1.178)
X−15523 levels	Keloids	IVW	46	0.046	1.111 (1.002 to 1.233)
Isovalerylglycine levels	Keloids	IVW	22	0.028	1.130 (1.013 to 1.261)
Indolelactate levels	Keloids	IVW	27	0.046	1.131 (1.002 to 1.276)
Adenosine 5'−diphosphate (ADP) to glycerol ratio	Keloids	IVW	21	0.030	1.137 (1.013 to 1.277)
Spermidine to ergothioneine ratio	Keloids	IVW	18	0.032	1.144 (1.012 to 1.293)
Taurolithocholate 3−sulfate levels	Keloids	IVW	21	0.047	1.160 (1.002 to 1.343)
P−cresol glucuronide levels	Keloids	IVW	23	0.023	1.164 (1.021 to 1.328)
Gulonate levels	Keloids	IVW	21	0.036	1.175 (1.010 to 1.367)
Proline to trans−4−hydroxyproline ratio	Keloids	IVW	25	0.014	1.175 (1.034 to 1.337)
Glucuronide of piperine metabolite C17H21NO3 (3) levels	Keloids	IVW	18	0.014	1.177 (1.034 to 1.339)
Myristoylcarnitine (C14) levels	Keloids	IVW	19	0.048	1.183 (1.002 to 1.397)
Sphingomyelin (d18:2/14:0, d18:1/14:1) levels	Keloids	IVW	20	0.040	1.194 (1.008 to 1.415)
Palmitoylcarnitine (C16) levels	Keloids	IVW	29	0.005	1.198 (1.055 to 1.361)
Phenylacetylglutamine levels	Keloids	IVW	19	0.030	1.198 (1.017 to 1.411)
4−hydroxyhippurate levels	Keloids	IVW	18	0.018	1.199 (1.031 to 1.394)
5−dodecenoate (12:1n7) levels	Keloids	IVW	15	0.028	1.213 (1.021 to 1.442)
3−hydroxy−3−methylglutarate levels	Keloids	IVW	21	0.009	1.219 (1.050 to 1.415)
Ornithine to phosphate ratio	Keloids	IVW	16	0.009	1.241 (1.055 to 1.461)
3−methyl−2−oxovalerate levels	Keloids	IVW	15	0.012	1.267 (1.054 to 1.524)
X−25957 levels	Keloids	IVW	19	<0.001	1.307 (1.115 to 1.531)
2,3−dihydroxy−2−methylbutyrate levels	Keloids	IVW	14	0.002	1.333 (1.107 to 1.606)
4−methyl−2−oxopentanoate levels	Keloids	IVW	12	<0.001	1.414 (1.178 to 1.697)

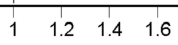

Figure 8 Forest plots of the association between metabolites and keloids. (**A**) Forest plot of 26 metabolites inhibiting keloids. (**B**) Forest plot of 23 metabolites promoting keloids.

Mediation	Outcome	Method	SNPs	MR.Pval	OR (95% CI)
Telomere Length	Keloids	IVW	207	0.002	1.252 (1.089 to 1.439)
PhenoAge	Keloids	IVW	11	0.023	0.925 (0.865 to 0.989)
GrimAge	Keloids	IVW	4	0.324	1.067 (0.938 to 1.214)
IEAA	Keloids	IVW	24	0.587	0.988 (0.945 to 1.033)

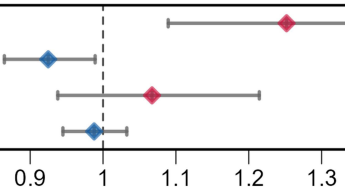

Figure 9 Forest plot of the association between ageing phenotypes and keloids.

[GCST90200660]) were ultimately identified as being related to keloid and involving telomere length. The Steiger's test results indicated no inverse causal relationship between these 87 metabolites and telomere length (Table S8). Sensitivity analysis validated the reliability of the MR results (Table S8).

PhenoAge

The 58 metabolites exhibiting potential causal relationships with PhenoAge were validated via MR analysis (Figure 5 and Table S7). Three of these metabolites also demonstrated significant effects on keloids but were excluded during directionality analysis (Figure S1). The remaining 55 metabolites could only influence keloids indirectly via PhenoAge. Steiger's test results indicated no reverse causality (Table S8). Tests for heterogeneity and multi-effect in the MR data confirmed their absence (Table S8).

Key Metabolites Screening in Biological Ageing

The intersection of metabolites causally linked to both telomere length and PhenoAge revealed two key mediators: Eugenol sulfate (GCST90199986) and Phenylacetylglutamate (GCST90200069) (Figure 10). These two metabolites positively correlated with keloid, indicating that the downregulation of these two metabolites may mitigate keloid development through promoting ageing. The mediation effect value of Eugenol sulphate on keloids via telomere length was 0.00336, while that via PhenoAge was 0.0222. The mediation effect value of Phenylacetylglutamate on keloids via telomere length is 0.00297, while the mediation effect value via PhenoAge is 0.0256 (Table 3). This implied that for each additional unit of Eugenol sulphate, the incidence of keloids mediated by telomere length increased by 0.336%, whilst the incidence mediated by PhenoAge increased by 2.22%. Similarly, for each additional unit of Phenylacetylglutamate, the incidence of keloids mediated by telomere length increases by 0.297%, while the incidence mediated by PhenoAge increases by 2.56%.

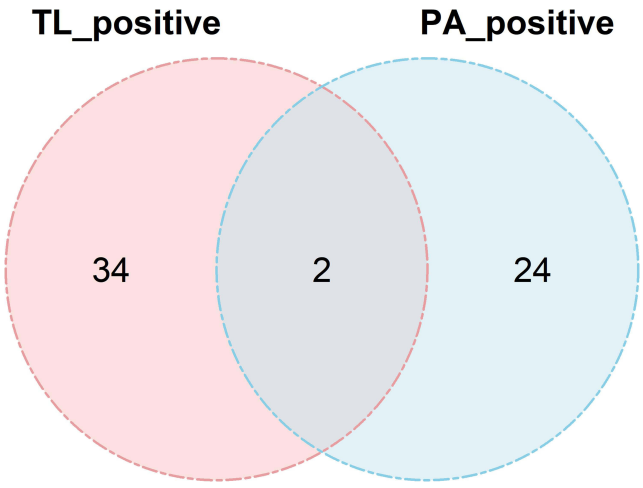

Figure 10 Venn diagram of the intersection metabolites with causal relationships to telomere length and PhenoAge.

https://doi.org/10.2147/CCID.S598554

Table 3 The Mediation Effect of 2 Key Metabolites Influencing Keloids

Exposure	Mediation	Outcome	Effect
Eugenol sulfate levels	Telomere length	Keloids	0.00336
Eugenol sulfate levels	PhenoAge	Keloids	0.0222
Phenylacetylglutamate levels	Telomere length	Keloids	0.00297
Phenylacetylglutamate levels	PhenoAge	Keloids	0.0256

Discussion

Scar formation following skin injury imposes both physical and psychological burdens on patients.[4] HS and keloids are common pathological scars with limited treatment efficacy. Specific metabolites may influence scar formation through ageing pathways. Therefore, we employed MR to investigate potential causal relationships among metabolites, ageing, HS, and keloids. Our core results demonstrated that among 1400 detected metabolites, 30 were causally associated with HS and 49 were causally associated with keloids. Mediation analysis revealed that 88 metabolites influence HS via telomere length, 58 metabolites affect HS through PhenoAge, while 63 metabolites exert indirect effects via IEAA. Moreover, 87 metabolites influence keloids via telomere length, while 58 metabolites affect keloids through PhenoAge. Eugenol sulfate and Phenylacetylglutamate exhibit potential causal relationships with both HS and keloids.

Ageing status presents closely correlated and heterogeneous associations with pathological scar risk. Existing observational studies indicated a negative correlation between HS incidence and age in patients undergoing breast reduction surgery or median sternotomy procedures.[28] In contrast, the peak incidence age for keloids is 20–29 years in males and 10–19 years in females. By age 60 and above, the incidence of keloids falls below 1% in both genders.[29] Ageing thus appears to exert a protective effect against scar formation. Consistent with this, our findings indicate that accelerated ageing constitutes a protective factor against HS/keloids. This protective mechanism may be explained by several factors: declining dermal cellular composition with age reduces proliferative capacity and diminishes skin regenerative potential. Reduced inflammatory response intensity in the elderly. The lower collagen I/III ratio in aged skin, coupled with disorganized collagen I arrangement, thus leads to cutaneous laxity.[30] In our study, we observed a significant positive correlation between the ageing marker telomere length and HS/keloids, and PhenoAge exhibited a significant negative causal relationship with HS/keloids, while GrimAge showed no potential causal link with HS/keloids. IEAA demonstrated a negative causal relationship with HS but no correlation with keloids. PhenoAge, GrimAge, and IEAA all belong to the category of epigenetic clocks, yet exhibit distinct causal relationships with HS/keloids. As we know, ageing is an exceedingly complex biological process, and different epigenetic clocks can only capture specific biological changes. The biological heterogeneity targeted by different ageing clocks probably explains the heterogeneity in their associations with HS/keloids.

Different ageing biomarkers present diverse mediating patterns in the metabolic regulation of pathological scars. Epigenetic clocks are established as quantitative models based on biomarkers, such as DNA methylation and proteomics, to measure an individual's biological age, which more accurately reflects functional status and disease risk than real age.[31] This study revealed stratified mediating patterns between metabolites and scarring across distinct ageing indicators through a multidimensional investigation of ageing indicators. Firstly, telomere length reflected cellular reproductive ageing. The metabolites glutathione and citrulline can influence telomerase activity.[32,33] Our study identified 88 metabolites, including glutathione and citrulline, that could affect HS/keloids via telomere length. We hypothesize that these metabolites may directly or indirectly modulate cellular telomerase activity. Secondly, PhenoAge was a comprehensive assessment of modifiable physiological indicators and Cytosine-phosphate-Guanine dinucleotide (CpG) island DNA methylation levels.[34] Our findings indicated that 58 metabolites influence HS/keloids via PhenoAge. Among these 58 metabolites, lauroylcarnitine and 3-hydroxyhexanoylcarnitine exhibited negative correlations with PhenoAge, thereby promoting HS/keloids. Lauryl carnitine and 3-hydroxyhexanoylcarnitine levels reflect fatty acid β-oxidation, indicating mitochondria can provide substantial energy for cellular activity. Myristoylcarnitine (C17) levels positively correlate with PhenoAge, inhibiting HS/keloids. Metabolism of myristoylcarnitine (C17) produces

propionyl-CoA, limiting mitochondrial tricarboxylic acid cycle energy production. Furthermore, sphingosine 1-phosphate promotes inflammation by activating the NF-κB pathway, thereby accelerating PhenoAge.[35] Hypothetically, these 58 metabolites primarily influence PhenoAge, and consequently HS/keloids, through metabolic reprogramming and inflammatory pathways. Thirdly, GrimAge primarily focuses on mortality-associated CpG sites,[36] hence showing no mediation effect. Finally, IEAA was an inherent epigenetic ageing rate of the genome after removing environmental interference.[37] Our findings indicated that the 63 metabolites, including pentose phosphate, exerted effects on HS via the IEAA pathway. Pentose phosphate, a product of the pentose phosphate pathway in carbohydrate metabolism, represents the metabolic status of the pentose phosphate pathway within cells. Pentose phosphate pathways provide key precursors for nucleic acid biosynthesis. These 63 metabolites might exert influence on DNA damage and repair through diverse mechanisms.

Eugenol sulfate and Phenylacetylglutamate are core-shared metabolites driving both HS and keloid pathogenesis. Among numerous metabolites, we found that Eugenol sulphate and Phenylacetylglutamate possessed the capabilities to influence HS and keloids via telomere length and PhenoAge. Eugenol, a naturally phenolic compound widely found in various plants, is extensively utilized in daily life as a component of fragrances, essential oils, and other applications. Eugenol could ameliorate skin photoageing in hairless mice by promoting skin extracellular matrix (ECM) deposition.[38] In this study, we found that Eugenol sulphate levels, as eugenol-related metabolites, could promote HS and keloids through anti-ageing effects. Avoiding the use and intake of foods and medications containing eugenol after injury or surgery could potentially reduce the occurrence of HS/keloids. Bacterial metabolites also play a crucial role in human health. Phenylalanine is metabolized by gut microbiota into phenylacetate, which is subsequently transported via the portal vein to the liver and converted into Phenylacetylglutamine.[39] Phenylacetylglutamate has been demonstrated to elevate intracellular reactive oxygen species levels via the adrenergic receptor-AMPK pathway, thereby promoting cellular senescence.[40] Moreover, Phenylacetylglutamine exhibits associations with multiple cardiovascular diseases.[41] Our research indicated that Phenylacetylglutamate may instead promote scar formation through anti-ageing mechanisms, suggesting a potential competitive relationship between Phenylacetylglutamate and Phenylacetylglutamine. This suggests that the topical application of Phenylacetylglutamine to competitively inhibit Phenylacetylglutamate may exert anti-scarring effects while avoiding systemic side effects.

Our results provide preliminary translational prospects for dietary, botanical and microbial metabolic interventions against pathological scars. Pharmaceutical formulations containing botanical components such as aloe vera gel, centella asiatica glycosides, green tea polyphenols, and onion extract demonstrated anti-scarring effects.[42] Our research also found that certain plant-derived metabolites, including vanillylmandelic acid and the piperine metabolite phosphate, inhibited HS or keloid formation. For instance, vanillic acid, one of the primary active components in the traditional Chinese herb picrorhizae rhizoma,[43] can combine with glycine to form vanillyl glycine, which inhibits HS and keloids. Our research provides clues for developing new plant-derived pharmaceutical formulations. Dietary intervention represents an affordable and feasible approach to metabolic modulation. After 6 weeks of consuming bran and navy beans, levels of metabolites related to tyrosine, cysteine, and leucine increased significantly.[44] In this study, metabolites associated with these three amino acids, 4-methoxyphenol sulphate, cysteine levels, and the leucine to N-palmitoyl-sphingosine (d18:1 to 16:0) ratio—exhibit a significant negative correlation with HS/keloids. Suppressing scarring by regulating metabolite levels through dietary adjustments is a viable approach. Our research findings demonstrated that not all short-chain fatty acids, secondary bile acids, or tryptophan derivatives exhibited inhibitory effects on HS and keloids, with certain metabolites paradoxically promoting fibrotic responses. This confirms the complexity and heterogeneity of microbiota-related metabolites. Nevertheless, our findings provide a theoretical framework for multidimensional metabolic interventions.

Our study revealed a potential causal relationship between circulating metabolites and HS/keloids, and explored the mediating role of multiple ageing indicators. In the near future, as more unknown circulating metabolites are detected and characterized, our research may continue to provide novel insights and inspiration. However, several limitations cannot be overlooked. Firstly, the core assumptions of MR analysis, including associativity, independence, and exclusivity, are difficult to fully validate, and residual pleiotropy may lead to biased causal estimates. Secondly, all GWAS data originated from European populations, raising questions about the generalizability of findings and potential limitations due to population heterogeneity. Thirdly, this study relies on genetic inference from public databases, lacking

experimental evidence to support specific biological mechanisms linking metabolites to ageing phenotypes. Fourthly, a large number of metabolites were tested simultaneously in this exploratory metabolome-wide MR analysis. Overly strict thresholds for IVs selection would substantially reduce eligible SNP numbers and weaken statistical power. Thus, appropriately relaxed criteria were adopted to ensure sufficient valid IVs. Although weak IVs were excluded by F-statistics, rare variants were filtered according to MAF, and comprehensive sensitivity analyses were performed, uncorrected multiple comparisons still inevitably elevate the risk of false-positive causal associations. Finally, although candidate metabolites were identified, the specific molecular mechanisms linking metabolites to ageing phenotypes, telomere homeostasis and epigenetic alterations, as well as subsequent fibroblast proliferation and ECM deposition, remain poorly elucidated. In summary, future research requires additional cross-ethnic, multicenter studies combined with experimental validation to further confirm and elucidate these findings.

Conclusion

In summary, this study employed MR methodology to reveal potential causal relationships between metabolites and HS/keloids. Specific blood metabolites, such as N-acetylglycine and eugenol sulfate, could not only directly influence the formation of pathological scars, including HS and keloids, but also exert indirect effects by regulating ageing phenotypes like telomere length and epigenetic age acceleration. Our findings indicate that metabolic dysregulation and biological ageing collectively constitute significant causal pathways affecting HS/keloids formation.

Abbreviation

HS, Hypertrophic scars; MR, Mendelian randomization; IVs, Instrumental variables; IEAA, Intrinsic Epigenetic Age Acceleration; GWAS, The Genome-Wide Association Study; LD, Linkage disequilibrium; Kb, kilobases; SNP, Single Nucleotide Polymorphisms; MAF, Minor allele frequencies; IVW, Inverse-variance weighted; ADP, Adenosine 5′-diphosphate; CpG, Cytosine-phosphate-Guanine dinucleotide; ECM, Extracellular matrix.

Data Sharing Statement

Data will be made available upon reasonable request.

Ethics Approval

The GWAS data utilized in this study consist of de-identified, publicly available datasets. In accordance with the Declaration of Helsinki (2024 revision) and local regulation—the Measures for the Ethical Review of Life Science and Medical Research Involving Humans (2023), studies using fully anonymized and publicly accessible data are exempt from additional ethical approval.

Acknowledgments

We would like to express our sincere gratitude to the IEU Open GWAS project and GWAS Catalog for providing the GWAS summary statistics essential for conducting our Mendelian randomization analyses. We are also deeply thankful to the researchers involved in the original studies and all the study participants whose contributions and efforts have made these valuable genetic resources accessible to the scientific community. Moreover, we gratefully acknowledge our colleague Qi Zhang for his contribution in polishing the language and conducting a grammatical review of this manuscript.

Author Contributions

Kang Wang and Kai Hou contributed equally to this work. All authors made a significant contribution to the work reported, whether that is in the conception, study design, execution, acquisition of data, analysis and interpretation, or in all these areas; took part in drafting, revising or critically reviewing the article; gave final approval of the version to be published; have agreed on the journal to which the article has been submitted; and agree to be accountable for all aspects of the work.

Funding

This work was supported by Hubei Provincial Natural Science Foundation of China (Grant No. 2023BCB088), Tongji Hospital Project (Grant No. 2024TJCR015) and Horizontal project funding (Grant No. 2025248).

Disclosure

The authors report no conflicts of interest in this work.

References

1. Madison KC. Barrier function of the skin: "la raison d'être" of the epidermis. *J Invest Dermatol*. 2003;121:231–241. doi:10.1046/j.1523-1747.2003.12359.x
2. Dąbrowska AK, Spano F, Derler S, Adlhart C, Spencer ND, Rossi RM. The relationship between skin function, barrier properties, and body-dependent factors. *Skin Res Technol*. 2018;24:165–174. doi:10.1111/srt.12424
3. Peña OA, Martin P. Cellular and molecular mechanisms of skin wound healing. *Nat Rev Mol Cell Biol*. 2024;25:599–616. doi:10.1038/s41580-024-00715-1
4. Hendriks TCC, Botman M, Binnerts JJ, et al. The development of burn scar contractures and impact on joint function, disability and quality of life in low- and middle-income countries: a prospective cohort study with one-year follow-up. *Burns*. 2022;48:215–227. doi:10.1016/j.burns.2021.04.024
5. Gauglitz GG, Korting HC, Pavicic T, Ruzicka T, Jeschke MG. Hypertrophic scarring and keloids: pathomechanisms and current and emerging treatment strategies. *Mol Med*. 2011;17:113–125. doi:10.2119/molmed.2009.00153
6. Liu S, Yang H, Song J, Zhang Y, Abualhssain ATH, Yang B. Keloid: genetic susceptibility and contributions of genetics and epigenetics to its pathogenesis. *Exp Dermatol*. 2022;31:1665–1675. doi:10.1111/exd.14671
7. Ogawa R, Okai K, Tokumura F, et al. The relationship between skin stretching/contraction and pathologic scarring: the important role of mechanical forces in keloid generation. *Wound Repair Regen*. 2012;20:149–157. doi:10.1111/j.1524-475X.2012.00766.x
8. Hong YK, Chang YH, Lin YC, Chen B, Guevara BEK, Hsu CK. Inflammation in wound healing and pathological scarring. *Adv Wound Care*. 2023;12:288–300. doi:10.1089/wound.2021.0161
9. Noishiki C, Hayasaka Y, Ogawa R. Sex differences in keloidogenesis: an analysis of 1659 keloid patients in Japan. *Dermatol Ther*. 2019;9:747–754. doi:10.1007/s13555-019-00327-0
10. Huang C, Ogawa R. Systemic factors that shape cutaneous pathological scarring. *FASEB J*. 2020;34:13171–13184. doi:10.1096/fj.202001157R
11. Frech FS, Hernandez L, Urbonas R, Zaken GA, Dreyfuss I, Nouri K. Hypertrophic scars and keloids: advances in treatment and review of established therapies. *Am J Clin Dermatol*. 2023;24:225–245. doi:10.1007/s40257-022-00744-6
12. Johnson CH, Ivanisevic J, Siuzdak G. Metabolomics: beyond biomarkers and towards mechanisms. *Nat Rev Mol Cell Biol*. 2016;17:451–459. doi:10.1038/nrm.2016.25
13. Li J, Zeng S, Zhang E, Chen L, Jiang J, Li J. Spatial metabolomics to discover hypertrophic scar relevant metabolic alterations and potential therapeutic strategies: a preliminary study. *Bioorg Chem*. 2024;153:107873. doi:10.1016/j.bioorg.2024.107873
14. Shan M, Liu H, Hao Y, et al. Metabolomic profiling reveals that 5-hydroxylysine and 1-methylnicotinamide are metabolic indicators of keloid severity. *Front Genet*. 2021;12:804248. doi:10.3389/fgene.2021.804248
15. Li W, Li X, Zhang Y, et al. Altered arginine metabolism affects proliferation and radiosensitivity of keloids. *Exp Dermatol*. 2025;34:e70077. doi:10.1111/exd.70077
16. Cai Y, Song W, Li J, et al. The landscape of aging. *Sci China Life Sci*. 2022;65:2354–2454. doi:10.1007/s11427-022-2161-3
17. Bucaciuc Mracica T, Anghel A, Ion CF, Moraru CV, Tacutu R, Lazar GA. MetaboAge DB: a repository of known ageing-related changes in the human metabolome. *Biogerontology*. 2020;21:763–771. doi:10.1007/s10522-020-09892-w
18. Panyard DJ, Yu B, Snyder MP. The metabolomics of human aging: advances, challenges, and opportunities. *Sci Adv*. 2022;8:eadd6155. doi:10.1126/sciadv.add6155
19. Yao C, Guan X, Carraro G, et al. Senescence of alveolar type 2 cells drives progressive pulmonary fibrosis. *Am J Respir Crit Care Med*. 2021;203:707–717. doi:10.1164/rccm.202004-1274OC
20. Docherty MH, Baird DP, Hughes J, Ferenbach DA. Cellular senescence and senotherapies in the kidney: current evidence and future directions. *Front Pharmacol*. 2020;11:–2020. doi:10.3389/fphar.2020.00755
21. O'Reilly S, Markiewicz E, Idowu OC. Aging, senescence, and cutaneous wound healing-a complex relationship. *Front Immunol*. 2024;15:1429716. doi:10.3389/fimmu.2024.1429716
22. Butzelaar L, Ulrich MM, Mink van der Molen AB, Niessen FB, Beelen RH. Currently known risk factors for hypertrophic skin scarring: a review. *J Plast Reconstr Aesthet Surg*. 2016;69:163–169. doi:10.1016/j.bjps.2015.11.015
23. Sanderson E, Glymour MM, Holmes MV, et al. Mendelian randomization. *Nat Rev Method Primers*. 2022;2:6. doi:10.1038/s43586-021-00092-5
24. Walker VM, Zheng J, Gaunt TR, Smith GD. Phenotypic causal inference using genome-wide association study data: mendelian randomization and beyond. *Annu Rev Biomed Data Sci*. 2022;5:1–17. doi:10.1146/annurev-biodatasci-122120-024910
25. Cheng X, Cheng B, Jin R, Zheng H, Zhou J, Shan S. The role of circulating metabolites and gut microbiome in hypertrophic scar: a two-sample Mendelian randomization study. *Arch Dermatol Res*. 2024;316:315. doi:10.1007/s00403-024-03116-8
26. Chen Y, Lu T, Pettersson-Kymmer U, et al. Genomic atlas of the plasma metabolome prioritizes metabolites implicated in human diseases. *Nat Genet*. 2023;55:44–53. doi:10.1038/s41588-022-01270-1
27. Hemani G, Zheng J, Elsworth B, et al. The MR-Base platform supports systematic causal inference across the human phenome. *eLife*. 2018;7. doi:10.7554/eLife.34408
28. Mahdavian Delavary B, van der Veer WM, Ferreira JA, Niessen FB, van der Veer WM. Formation of hypertrophic scars: evolution and susceptibility. *J Plast Surg Hand Surg*. 2012;46:95–101. doi:10.3109/2000656X.2012.669184

29. Lu W-S, Zheng X-D, Yao X-H, Zhang L-F. Clinical and epidemiological analysis of keloids in Chinese patients. *Archives of Dermatological Res*. 2015;307:109–114. doi:10.1007/s00403-014-1507-1
30. Enoch S, Price P. Cellular, molecular and biochemical differences in the pathophysiology of healing between acute wounds, chronic wounds and wounds in the aged. *World Wide Wounds*. 2004;13:1–7.
31. Teschendorff AE, Horvath S. Epigenetic ageing clocks: statistical methods and emerging computational challenges. *Nat Rev Genet*. 2025;26:350–368. doi:10.1038/s41576-024-00807-w
32. Borrás C, Esteve JM, Viña JR, Sastre J, Viña J, Pallardó FV. Glutathione regulates telomerase activity in 3T3 fibroblasts. *J Biol Chem*. 2004;279:34332–34335. doi:10.1074/jbc.M402425200
33. Tsuboi T, Maeda M, Hayashi T. Administration of L-arginine plus L-citrulline or L-citrulline alone successfully retarded endothelial senescence. *PLoS One*. 2018;13:e0192252. doi:10.1371/journal.pone.0192252
34. Levine ME, Lu AT, Quach A, et al. An epigenetic biomarker of aging for lifespan and healthspan. *Aging*. 2018;10:573–591. doi:10.18632/aging.101414
35. Chung HL, Ye Q, Park YJ, et al. Very-long-chain fatty acids induce glial-derived sphingosine-1-phosphate synthesis, secretion, and neuroinflammation. *Cell Metab*. 2023;35:855–74.e5. doi:10.1016/j.cmet.2023.03.022
36. Lu AT, Quach A, Wilson JG, et al. DNA methylation GrimAge strongly predicts lifespan and healthspan. *Aging*. 2019;11:303–327. doi:10.18632/aging.101684
37. Horvath S, Raj K. DNA methylation-based biomarkers and the epigenetic clock theory of ageing. *Nat Rev Genet*. 2018;19:371–384. doi:10.1038/s41576-018-0004-3
38. Tong T, Geng R, Kang SG, Li X, Huang K, Jeon E-J. Revitalizing photoaging skin through eugenol in UVB-exposed hairless mice: mechanistic insights from integrated multi-omics. *Antioxidants*. 2024;14:13. doi:10.3390/antiox14010013
39. Song Y, Wei H, Zhou Z, et al. Gut microbiota-dependent phenylacetylglutamine in cardiovascular disease: current knowledge and new insights. *Front Med*. 2024;18:31–45. doi:10.1007/s11684-024-1055-9
40. Yang H, Wang T, Qian C, et al. Gut microbial-derived phenylacetylglutamine accelerates host cellular senescence. *Nat Aging*. 2025;5:401–418. doi:10.1038/s43587-024-00795-w
41. Nemet I, Saha PP, Gupta N, et al. A cardiovascular disease-linked gut microbial metabolite acts via adrenergic receptors. *Cell*. 2020;180:862–77.e22. doi:10.1016/j.cell.2020.02.016
42. Prananda AT, Nugraha SE, Situmorang PC, Syahputra RA. Comparative effectiveness of plant-derived compounds in keloid management: a review. *Front Pharmacol*. 2025;16:1576851. doi:10.3389/fphar.2025.1576851
43. Wu J, Song Z, Cai N, et al. Pharmacokinetics, tissue distribution and excretion of six bioactive components from total glucosides picrorhizae rhizoma, as simultaneous determined by a UHPLC-MS/MS method. *J Chromatogr B Analyt Technol Biomed Life Sci*. 2023;1227:123830. doi:10.1016/j.jchromb.2023.123830
44. Hill EB, Baxter BA, Pfluger B, et al. Plasma, urine, and stool metabolites in response to dietary rice bran and navy bean supplementation in adults at high-risk for colorectal cancer. *Front Gastroenterol*. 2023;2. doi:10.3389/fgstr.2023.1087056